Epigenetic changes in histone H3 modification of Cat-Cow interspecies cloned embryos after treatment with the histone deacetylase inhibitor Trichostatin A

Running head: Histone H3 modification of iSCNT cat-cow embryos after TSA treatment

Manita Wittayarat[a,b], Yoko Sato[a*], Lanh Thi Kim Do[a], Kaywalee Chatdarong[b], Theerawat Tharasanit[b], Mongkol Techakumphu[b], Masayasu Taniguchi[a], Takeshige Otoi[a]

[a]The United Graduate School of Veterinary Science, Yamaguchi University, Yamaguchi 753-8515, Japan

[b]Department of Obstetrics, Gynaecology and Reproduction, Faculty of Veterinary Sciences, Chulalongkorn University, Bangkok 10330, Thailand

*Corresponding author, present address: Department of Medical Engineering, Faculty of Allied Sciences, University of East Asia, Shimonoseki, 751-8503, Japan
Tel: +81-83-257-5152
E-mail address: pxx13340@nifty.ne.jp

Abstract

This study aimed to determine the acetylation patterns on histone H3K9/18/23 and the dimethylation pattern on histone H3K9 during early embryogenesis among 50 nM Trichostatin A (TSA)-treated iSCNT cat-cow embryos, untreated iSCNT cat-cow embryos (control) and bovine *in vitro* fertilisation (IVF) embryos, because TSA-treated iSCNT embryos are able to develop into blastocysts. The results show that the acetylation levels of H3K9/18/23 in the TSA-treated iSCNT and bovine IVF embryos were higher than those in the control embryos at almost all of the examined stages (2 h post-fusion / post-insemination (PF/PI), pronuclear (PN), two-cell, four-cell and eight-cell stages). At 6 h PF/PI the acetylation levels on H3K9/23 in the TSA-treated iSCNT and bovine IVF embryos were lower than those in the control, and there was no difference in the acetylation levels of H3K18 among the three groups. The acetylation levels of H3K9/23 increased either in the TSA-treated iSCNT or and bovine IVF embryos increased when those embryos developed to the PN and two-cell stages. The dimethylation level of H3K9 in the TSA-treated iSCNT embryos resembled that of the bovine IVF embryos at all examined stages (2h PF/PI, 6 h PF/PI and PN stages), and these levels were greater than those of the control. This result suggests that treatment of iSCNT embryos with TSA modifies the patterns of histone acetylation and dimethylation at certain lysine residues in a manner that is comparable with that seen in IVF embryos during early embryogenesis.

Keywords: acetylation, cat, cow, histone, interspecies nuclear transfer, methylation, Trichostatin A

Introduction

Interspecies somatic cell nuclear transfer (iSCNT) has been developed for the purpose of endangered animal conservation as well as for analysing the interactions between the donor nucleus and the recipient cytoplasm (Yamochi et al., 2012); however, incomplete nuclear reprogramming, a low blastocyst rate, and abnormal epigenetic reprogramming are still major problems of this technique (Shi et al., 2008; Wu et al., 2011). Histone modifications play important roles in cell growth, cell cycle control, development, differentiation and survival during embryonic development (Gray and Dangond, 2006; Lee et al., 2010) through the binding interactions of the acetyl or methyl groups in the amino-terminal tail of core histones (Suteevun et al., 2006). Cloned embryos usually show higher rate of abnormal patterns of histone modification on developmental embryos (Liu et al., 2012; Wu et al., 2011), therefore, the normal patterns of histone modification are thought to be required for the development of cloned embryos (Maalouf et al., 2009; Shi et al., 2008; Zhao et al., 2009). Several researchers have investigated the mechanism underlying aberrant epigenetic information, which can lead to the deregulation of a number of important gene expressions in cloned embryos (Maalouf et al., 2008). For example, to adjust the patterns of histone acetylation in cloned embryos to be similar to those of normal embryos, the treatment of early stage embryos with a histone deacetylase (HDAC) inhibitor, such as Trichostatin A (TSA), has been suggested (Lee et al., 2010).

The deacetylation of core histones by HDAC leads to transcriptional repression (Pazin and Kadonaga, 1997) by catalysing the removal of acetyl groups from the epsilon-amino groups of distinct lysine residues in the amino-terminal tail of core histones (Finnin et al., 1999; Tribus et al., 2005). The HDAC inhibitors TSA and n-butyrate can cause the accumulation of highly acetylated histone species within cells, resulting in a variety of phenotypic changes (Liu et al., 2012; Nakajima et al., 1998). The ability of TSA to increase the *in vitro* embryo developmental rate has been demonstrated in a number of SCNT studies, e.g. in pigs (Li et al., 2008; Zhang et al., 2007), mice (Kishigami et al., 2006) and cattle (Sawai et al., 2012). Acetylation at lysine 9 and lysine 18 of histone H3 (H3K9ac and H3K18ac) has crucial roles in activating gene transcription (Pham et al., 2007; Sawai et al., 2012). Concurrently, the

acetylation at lysine 23 of histone H3 (H3K23ac) can regulate the recognition of the chromodomain of polycomb proteins (Robin et al., 2007), which is essential for gene expression during development in mammals (Ku et al., 2008). Moreover, H3K18ac and H3K23ac have been considered to play an important role for ordered oocyte meiosis (Xue et al., 2010); however, very few studies have investigated the dynamics of several acetylated lysine residues in iSCNT embryos during early embryogenesis after fusion (Gómez et al., 2011; Shi et al., 2008). Additionally, the methylation of lysine residues displays the highest degree of complexity among known covalent histone modifications (McGraw et al., 2003). Histone lysine methylation has different effects depending on the residue that is methylated. The dimethylation on K9 of histone H3 (H3K9me2) and tri-methylation on K27 of histone H3 (H3K27me3) are generally correlated with transcriptional repression (Jin et al., 2011; Robin et al., 2007). In contrast, tri-methylation on K4 and K36 of histone H3 (H3K4me3 and H3K36me3) is associated with gene activation (Jin et al., 2011).

Nuclei from somatic cells of the domestic cat could be reprogrammed when transferred into bovine oocytes; however, the embryos were not able to develop beyond the eight-cell stage without any treatment for epigenetic modification (Thongphakdee et al., 2008). This developmental block might be caused by aberrant epigenetic patterns before embryonic genome activation, the most important event during early development for embryo viability (Meirelles et al., 2004). Furthermore, genomic activation among the embryo species differs in timing; embryonic genomic activation occurs at the five- to eight-cell stage in the domestic cat (Hoffert et al., 1997) and the eight- to sixteen-cell stage in the cow (Camous et al., 1986). Previously, we showed that the treatment of iSCNT cat-cow embryos with TSA at concentration 50 nM for 24 h after fusion could support embryo development until the blastocyst stage, whereas none of the un-treated iSCNT cat embryos developed beyond the eight- to- sixteen-cell stage (Wittayarat et al., 2013). Therefore, the assessment of the covalent patterns of acetylation and methylation on histone H3 might be valuable to determine its role on early iSCNT cloned cat embryo development to improve the culture condition of the embryos. In the present study, we demonstrate the covalent patterns of H3K9/18/23ac and H3K9me2 in iSCNT cat embryos treated with 50 nM TSA compared to un-treated iSCNT embryos (control) and *in vitro* fertilised bovine embryos during early embryogenesis, including before cleavage.

Materials and Methods

Preparation of recipient oocytes and domestic cat somatic cells for nuclear transfer

Bovine oocytes were matured according to procedures described previously by Mori *et al*. (Mori et al., 2002). Cumulus-oocyte complexes (COCs) were cultured in maturation medium that consisted of TCM 199 with Earle's salts (Invitrogen, Carlsbad, CA, USA) supplemented with 0.05 g of taurine (Sigma-Aldrich, St. Louis, MO, USA), 0.02 IU/mL of follicle stimulating hormone (FSH; Kawasaki Mitaka Seiyaku K.K., Kawasaki, Japan), 5% foetal bovine serum (FBS; Invitrogen), 40 μg/mL of epidermal growth factor (EGF; Sigma-Aldrich), and 50 μg/mL of gentamicin (Sigma-Aldrich) for 22 h at 38.5°C in a humidified atmosphere containing 5% CO_2.

Domestic cat fibroblast cells were cultured in Dulbecco's modified Eagle's medium (DMEM; Invitrogen) supplemented with 20% (v/v) FBS and 50 μg/mL of gentamicin at 37°C in a humidified atmosphere containing 5% CO_2. Once the fibroblast cells reached complete confluence, the cells were trypsinised with 0.25% (w/v) trypsin (Invitrogen). Afterwards, the cells were either frozen for storage or used as donors for nuclear transfer (passage 3-6) (Kaedei et al., 2010).

SCNT, activation, in vitro culture of embryos, and TSA treatment

SCNT was conducted according to the methods previously described by Taniguchi et al. (Taniguchi et al., 2007). Briefly, the zona pellucida above the first polar body was cut with a glass needle and a small volume of cytoplasm was then squeezed out (the metaphase spindle and first polar body were visualised after incubating the oocytes in 3 μg/mL of Hoechst 33342 (Sigma-Aldrich)). A single cat cell was then introduced into the perivitelline space of the enucleated oocyte. The couplets were fused and activated simultaneously with a single DC pulse of 2.3 kV/cm for 30 μs delivered by two electrode needles (LF101; Nepa Gene Co. Ltd., Chiba, Japan) connected to a micromanipulator (MO-202D; Narishige Co. Ltd., Tokyo, Japan). The fused couplets were cultured for 5 h in a modified synthetic oviduct fluid (mSOF) medium (Kwun et al., 2003) supplemented with 10 μg/mL of cycloheximide (Sigma-Aldrich) and 50 nM TSA (Wako Pure Chemical Industries. Ltd., Tokyo, Japan). The fused embryos were then transferred to mSOF medium

containing 50 nM TSA and cultured for an additional 19 h. After 24 h of TSA treatment, the embryos were cultured in mSOF medium supplemented with 4 mg/mL of bovine serum albumin (BSA; Sigma-Aldrich) for 2 days at 38.5°C in a humidified atmosphere of 5% CO_2, 5% O_2 and 90%N_2. The embryos cultured without TSA treatment served as the control. To determine the covalent patterns of H3K9/18/23ac and H3K9me2, the embryos were collected at 2 h post-fusion (PF), 6 h PF, 20 h PF (pronuclear; PN), 24 h PF (two-cell), and day 3 of culture (four- and eight-cell).

To compare with naturally fertilised embryos, *in vitro* fertilised (IVF) bovine embryos were used. IVF was carried out according to the method described by Taniguchi et al. (Taniguchi et al., 2007). The PN and two-cell stage embryos were collected at 20 h and 24 h post-insemination (PI), respectively, and the four- and eight-cell stage embryos were collected at 48 h PI for fluorescent immunodetection.

Fluorescent immunodetection of H3K9ac, H3K18ac, H3K23ac and H3K9me2 in iSCNT cloned cat embryos

Fluorescent immunodetection was processed according to the protocol described in our previous study (Wittayarat et al., 2013). The embryos at 2 h PF/PI, 6 h PF/PI, PN, two-cell, four-cell and eight-cell stages from the 50 nM TSA-treated, control and IVF groups were subjected to H3K9ac, H3K18ac and H3K23ac fluorescent immunodetection. Simultaneously, the embryos at 2 h PF/PI, 6 h PF/PI and PN stages were used for H3K9me2 fluorescent immunodetection because the change of the H3K9/18/23ac was high during these periods.

All of the following steps were performed at room temperature (RT) and all of the solutions were prepared in 10% FBS/phosphate-buffered saline (PBS), unless otherwise indicated. The embryos were fixed in 3.7% paraformaldehyde/PBS overnight at 4ºC, permeabilised with 0.1% TritonX-100 (Sigma-Aldrich)/PBS for 40 min and then stored in 1% (w/v) BSA/PBS overnight at 4°C. The permeabilised embryos were incubated in 10% goat serum (Nichirei, Tokyo, Japan)/PBS for 1 h to block non-specific binding before incubated with the following primary antibodies; rabbit polyclonal acetyl-histone H3K9 antibody (5 μg/ml), H3K18 antibody (1.4 μg/ml), H3K23 antibody (2.7 μg/ml), rabbit polyclonal di-methyl-histone H3K9 antibody (5 μg/ml) or rabbit polyclonal histone H3 antibody (5 μg/ml), (Cell Signaling Technology Inc., Danvers, MA, USA) respectively in a moisture chamber overnight at RT. Normal rabbit immunoglobulin G (IgG; Dako, Kyoto, Japan)

adjusted to the same concentration of primary antibodies, was used as the negative control. The embryos were subsequently incubated in 4 μg/ml of Alexa 594-conjugated goat anti-rabbit IgG secondary antibody (Invitrogen) for 1 h in a moisture chamber before counterstained with 5 μg/ml of 4', 6-diamidino-2-phenylindole (DAPI; Invitrogen) for 10 min in the dark. The images were obtained using a fluorescence microscope (Nikon Eclipse 80i; Nikon, Tokyo, Japan) equipped with a Nikon DS-Ri1 digital camera (Nikon). The images were then acquired using the NIS-Element D 3.1 (Nikon) imaging software package running on a work station (Dell Optiplex 960 PC; Dell Inc., Austin, TX, USA).

Semi-quantification of fluorescence intensities in the embryos

The fluorescence images of each nucleus within an embryo were taken under the following conditions: Alexa Fluor 594 dye, DAPI, and in the bright field. The signal intensities of fluorescence from acetylated histone H3K9/18/23ac, dimethylated histone H3K9me2, histone H3 and DAPI-nucleic acid staining were measured automatically using imaging software under the area of the nucleus by manually outlining a limited area of each nucleus within an embryo, except for overlapping or folded nuclei. The fluorescence intensities of the embryonic cytoplasm and background were quantified using the same method. The mean intensity in each examined nucleus was recorded. The relative intensity levels of H3K9/18/23ac and H3K9me2 in each nucleus were calculated using the following formula.

$$\text{Relative intensity in one nucleus} = \frac{\text{H3K9/18/23ac or H3K9me2 (Mean intensity of nucleus - mean intensity of cytoplasm)}}{\text{DAPI (Mean intensity of nucleus- mean intensity of cytoplasm)}}$$

The relative intensity levels of histone H3 in each nucleus were also calculated using the same formula. Subsequently, the average values of relative intensity levels of H3K9/18/23ac, H3K9me2 and histone H3 in each embryo were calculated. These average values of each embryo were used for additional calculations to ascertain the average value of the relative intensity levels of H3 K9/18/23ac, H3K9me2 and histone H3 in each treatment. The data compensation, in each treatment, during the experiments was performed using the average value of the relative intensity levels of H3K9/18/23ac, H3K9me2 and histone H3 in the control samples without TSA treatment.

Statistical analysis

The percentage data of the intensity levels of H3K9/18/23ac, H3K9me2 and histone H3 in the embryos were subjected to arc-sin transformation before analysis of variance (ANOVA). The transformed data were tested by the Kruskal–Wallis test, followed by Fisher's protected least significant difference (PLSD) *post hoc* test. Differences with a probability value *(p)* of 0.05 or less were considered statistically significant.

Results

All of the nuclei of the iSCNT cloned cat embryos and bovine IVF at any of the examined stages showed positive immuno-reactivity in acetyl-histone H3K9, H3K18, H3K23 and di-methyl-histone H3K9, irrespective of the TSA treatment (Figs. 1A-D). The levels of histone H3 in the embryos were similar in all of the embryonic stages among the three groups (control, TSA treated and IVF) (Figs. 2A-D). No differences were found in the histone H3 levels in the embryos among the embryonic stages, irrespective of the TSA treatment (Figs. 1E, 2E).

Characterisation of H3K9ac, H3K18ac and H3K23ac in iSCNT cat embryos with or without treatment with 50 nM TSA post-fusion for 24 h in comparison with bovine IVF embryos

The levels of H3K9/18/23ac in TSA-treated iSCNT embryos, un-treated iSCNT (control) embryos and bovine IVF embryos were evaluated (Figs.1A-C, 2A-C). The fluorescence intensities in H3K9ac of the control embryos were significantly lower than those of the TSA-treated iSCNT embryos in almost all of the examined stages ($p < 0.05$) (Figs. 1A, 2A) except for 6 h PF, where the levels of H3K9ac in the TSA-treated iSCNT embryos (0.99 ± 0.05) were significantly lower than those of the control embryos (2.82 ± 0.17). The nuclear fluorescence intensities of H3K9ac in the TSA-treated iSCNT embryos at PN, four- and eight-cell stages did not show any significant difference compared to those of the bovine IVF embryos at the same stage. A significantly higher ($p < 0.05$) intensity of H3K9ac was observed in the TSA-treated iSCNT embryos at the two-cell stage, whereas, an apparently lower ($p < 0.05$)

intensity of acetylation at this residue was found either at 2 h PF or 6 h PF compared to the bovine IVF embryos.

The signal intensities of H3K18ac in the TSA-treated iSCNT embryos and bovine IVF embryos were also significantly higher than those of the control embryos at almost all of the examined stages ($p < 0.05$) (Figs. 1B, 2B), except for the 6 h PF stage where the signal levels were similar among the groups. At the PN stage, the nuclear fluorescence intensity of H3K18ac in the TSA-treated iSCNT embryos was significantly higher ($p < 0.05$) than those of the bovine IVF embryos. In contrast, a significantly lower intensity ($p < 0.05$) of H3K18ac was observed at the 2 h PF and four-cell stage in the TSA-treated iSCNT embryos compared with the bovine IVF embryos.

For the H3K23ac levels, bovine IVF and TSA-treated iSCNT embryos expressed lower levels than the control embryos at the 6 h PF/PI stages ($p < 0.05$) (Figs. 1C, 2C). Additionally, significantly higher signal levels of H3K23ac at the PN and eight-cell stages were observed in the TSA-treated iSCNT and bovine IVF embryos compared with those of the control embryos ($p < 0.05$). No significant differences were observed in H3K23ac levels among the three groups at the 2 h PF/PI, two- and four-cell stages.

Characterisation of H3K9me2 in iSCNT cat embryos with or without treatment of 50 nM TSA post-fusion for 24 h in comparison with bovine IVF embryos

The levels of H3K9me2 were determined in both the iSCNT cat embryos with or without (control) treatments with 50 nM TSA and the bovine IVF embryos (Fig. 1D, 2D). The TSA-treated iSCNT embryos showed significantly higher intensity levels of H3K9me2 than those of the control embryos and have resembled that of the bovine IVF at all of the examined stages (2 h PF, 6 h PF and PN stages) ($p < 0.05$) .

Discussion

In the present study, we investigated the histone modifications on various lysine residues in iSCNT embryos both before and after cleavage to understand the role of TSA in the improved development of iSCNT cat embryos, because treatment with 50 nM TSA after fusion of the couplets between bovine recipient cytoplasts and cat donor cells for 24 h is beneficial for development to the blastocyst stage (Wittayarat et al., 2013). Maternal and zygotic epigenetic factors play essential roles

during the development of a pre-implantation embryo and each stage has its own characteristic modified histone profile (Shi and Wu, 2009). In iSCNT embryos, somatic cells and zygotic histone modifications should occur in a similar condition as those in IVF embryos after their fusion for further development. Here we showed that the acetylation levels on H3K9, H3K18 and H3K23 of the TSA-treated embryos were modified to similar levels as the bovine IVF embryos, which was significantly different from the control (untreated iSCNT) embryos, with the exception of some specific stages. The results suggest that the treatment with TSA modified the acetylation levels on each lysine residue of the iSCNT cat embryos during early development after fusion.

Interestingly, the modification profile of each residue before pronuclear formation differed depending on the timing. At 2 h PF/PI, the acetylation levels of both H3K9 and H3K18 in both the TSA-treated embryos and bovine IVF embryos were significantly greater than those in the control embryos. Our results regarding acetylated H3K9 levels have confirmed the report by Gómez et al. (2011) that TSA treatment increased the acetylation levels in interspecies black-footed cat cloned embryos at 2 h after SCNT, which is similar to the increase seen in the nuclei of cat IVF embryos; however, there were no differences among the groups in the acetylation levels of H3K23. Others have suggested that there were differences in the affected genes because of the various sites of histone acetylation (Pham et al., 2007; Robin et al., 2007; Sawai et al., 2012). Thus, the proposed gene affected by the acetylation of H3K23 might be dispensable for embryo development at 2 h PF/PI, because the IVF embryo showed the same acetylation levels on this residue as the iSCNT embryos.

Furthermore, at 6 h PF/PI, the acetylation levels on H3K9 and H3K23 of the TSA-treated iSCNT embryos and bovine IVF embryos were significantly lower than those of the control embryos, suggesting that repression of the gene expression related to these residues might be required at the 6 h PF/PI stage; however, there was a different acetylation levels between these two acetylation sites. Of note, the change in the acetylation levels of H3K9 include de-acetylation between 2-6 h PF/PI and hyper-acetylation between 6 h PF/PI to PN formation; however, the acetylation levels of H3K23 increased gradually until PN formation and did not reveal any de-acetylation. The transient de-acetylation on certain histone lysine residues between 2-6 h PI/PF, which has already been reported in cat IVF (Gomez et al., 2011), mouse NT (Kim et al., 2003; Rybouchkin et al., 2006; Wang et al., 2007) and rabbit NT (Shi et al., 2008),

might be considered a crucial event for further development of the iSCNT embryo. This event is possibly associated with a rapid loss of the maturation-promoting factor and the mitogen-activated protein kinase activities in the matured metaphase II oocytes, as well as to allow the transferred somatic genome to exhibit an acetylation level similar to the oocyte chromosomes (Wang et al., 2007). De-acetylation of H3K9 in the iSCNT embryo might also be important in the nuclear reprogramming process and the initiation of the zygotic gene expression program to erase the somatic cell memory and create a relatively naive chromatin state, similar to the mouse NT and Rabbit NT (Kim et al., 2003; Shi et al., 2008); however, the acetylation level of H3K18 was quite high in all of the groups at the 6 h PF/PI stage. The gene expression related to the H3K18 residue would be promoted in all of the embryo groups, and the acetylation level of this residue at the 6 h PF/PI stage was not affected by the TSA treatment. These results suggest that histone deacetylation at specific lysine residues occurred before the formation of the pronucleus, despite the increase in global histone acetylation (Rybouchkin et al., 2006; Shi et al., 2008).

The present study showed that the high levels of acetylation on H3K9/18/23 were observed in the TSA-treated iSCNT group either at the PN or two-cell stage, which resembles the bovine IVF group in this study and is in agreement with previous studies in the mouse, sheep, cat and miniature pig (Gomez et al., 2011; Hou et al., 2008; Yamanaka et al., 2009). The hyper-acetylation at several lysine residues of histone (H3K9/18/23) by TSA might promote the development of the blastocyst from an iSCNT embryo, as we reported previously (Wittayarat et al., 2013), because TSA would re-establish the embryonic epigenetic characteristics and gene expression within a limited time (PN to two-cell stage) (Shi et al., 2008; Wu et al., 2011) for an easier entry of some essential transcriptional factors into the nucleosome to activate gene expression (Lee et al., 1993; Yamanaka et al., 2009), stimulating more effective remodelling of the somatic chromatin (Rybouchkin et al., 2006). Subsequently, a decrease in the acetylation on each residue was observed after hyper-acetylation at the PN to the 2- or 4-cell stage. This gradual depletion of acetylation levels on H3K9/18/23 in the TSA-treated iSCNT and bovine IVF groups might have resulted from the dynamic change in GCN5, a ubiquitous histone acetyltransferase (Schiltz et al., 1999; Wu et al., 2010). High levels of GCN5 transcripts occur in the bovine germinal vesicle (GV), MII oocytes and two-cell stage embryos before markedly decreasing at the eight-cell stage (McGraw et al., 2003). The end point of TSA

treatment at 24 h may possibly inhibit the hyper-acetylation after development beyond the two-cell stage, resulting in the consistent decrease in acetylation levels with the dynamic change of GCN5; however, to understand the mechanism of the decrease in the acetylation levels, the assessment of GCN5 levels or other candidate molecule levels throughout embryonic development should be carried out.

The methylation of H3K9, catalysed by histone methyltransferases (HMTs) (Rice and Allis, 2001), generally correlates with transcriptional repression (Robin et al., 2007). Factors present in the recipient cytoplast are responsible for inducing de-methylation of the transferred nucleus and the process is not species-specific (Gomez et al., 2011). We have observed that the H3K9me2 levels through early embryo development (2 h PF to PN stages) of the TSA-treated iSCNT embryos and bovine IVF embryos are apparently higher than that of the control embryos. Perhaps this phenomenon could be associated with the requirement for de-acetylation of H3K9 at 6 h PF/PI. Methylation and acetylation of histone residues collaborate to control both gene transcription and repression, and the acetylation levels of histone residues is thought to be regulated by some sites of histone methylation (Rice and Allis, 2001). The de-acetylation of lysine 9 may serve to suppress transcriptionally competent regions of the genome by inducing methylation of lysine 9 and preventing the upstream assembly of heterochromatin (Rice and Allis, 2001). This suggests that, under TSA treatment, bovine cytoplasm was able to alter the de-methylation of chromatin in the cat donor cell to a sufficient level such that the de-acetylation could not occur at 6 h PF.

In conclusion, the treatment of iSCNT cat embryos with 50 nM TSA for 24 h after fusion provides beneficial effects regarding the modification of the acetylation levels of lysines 9, 18, 23 and the di-methylation level of lysine 9 on histone H3 in early embryogenesis, although the acetylation patterns may differ among the lysine residues. We suggest that the patterns of acetylation on H3K9/18/23 and di-methylation on H3K9 induced by TSA in the present study were sufficient to resemble those of naturally fertilised embryos, leading to improvements in the *in vitro* development of iSCNT cat-cow embryos.

Acknowledgements

The authors express their gratitude to the staff of the Meat Inspection Office of Kitakyushu City, Japan, for supplying bovine ovaries. This study was supported in

part by a grant from the Ministry of Education, Culture, Sports, Science and Technology to T.O. (22580320).

Author Disclosure Statement

No competing financial interests exist.

References

Camous, S., Kopecny, V. and Flechon, J.E. (1986). Autoradiographic detection of the earliest stage of [3H]-uridine incorporation into the cow embryo. Biol Cell. 58, 195-200.

Finnin, M.S., Donigian, J.R., Cohen, A., et al. (1999). Structures of a histone deacetylase homologue bound to the TSA and SAHA inhibitors. Nature. 401, 188-193.

Gómez, M.C., Pope, C.E., Biancardi, M.N., et al. (2011). Trichostatin A modified histone covalent pattern and enhanced expression of pluripotent genes in interspecies black-footed cat cloned embryos but did not improve in vitro and in vivo viability. Cell Reprogram. 13, 315-329.

Gray, S.G. and Dangond, F. (2006). Rationale for the use of histone deacetylase inhibitors as a dual therapeutic modality in multiple sclerosis. Epigenetics. 1, 67-75.

Hoffert, K.A., Anderson, G.B., Wildt, D.E., et al. (1997). Transition from maternal to embryonic control of development in IVM/IVF domestic cat embryos. Mol Reprod Dev. 48, 208-215.

Hou, J., Liu, L., Zhang, J., et al. (2008). Epigenetic modification of histone 3 at lysine 9 in sheep zygotes and its relationship with DNA methylation. BMC Develo Biol. 8, 60.

Jin, Q., Yu, L.R., Wang, L., et al. (2011). Distinct roles of GCN5/PCAF-mediated H3K9ac and CBP/p300-mediated H3K18/27ac in nuclear receptor transactivation. EMBO J. 30, 249-262.

Kaedei, Y., Fujiwara, A., Tanihara, F., et al. (2010). In vitro development of cat interspecies nuclear transfer using pig's and cow's cytoplasm. Bull Vet Inst Pulawy. 54, 405-408.

Kim, J.M., Liu, H., Tazaki, M., et al. (2003). Changes in histone acetylation during mouse oocyte meiosis. J Cell Biol. 162, 37-46.

Kishigami, S., Mizutani, E., Ohta, H., et al. (2006). Significant improvement of mouse cloning technique by treatment with trichostatin A after somatic nuclear transfer. Biochem Biophys Res Commun. 340, 183-189.

Ku, M., Koche, R.P., Rheinbay, E., et al. (2008). Genomewide analysis of PRC1 and PRC2 occupancy identifies two classes of bivalent domains. PLoS Genet. 4, e1000242.

Kwun, J., Chang, K., Lim, J., et al. (2003). Effects of exogenous hexoses on bovine in vitro fertilized and cloned embryo development: Improved blastocyst formation after glucose replacement with fructose in a serum-free culture medium. Mol Reprod Dev. 65, 167-174.

Lee, D.Y., Hayes, J.J., Pruss, D., et al. (1993). A positive role for histone acetylation in transcription factor access to nucleosomal DNA. Cell. 72, 73-84.

Lee, H.S., Yu, X.F., Bang, J.I., et al. (2010). Enhanced histone acetylation in somatic cells induced by a histone deacetylase inhibitor improved inter-generic cloned leopard cat blastocysts. Theriogenology. 74, 1439-1449.

Li, J., Svarcova, O., Villemoes, K., et al. (2008). High in vitro development after somatic cell nuclear transfer and trichostatin A treatment of reconstructed porcine embryos. Theriogenology. 70, 800-808.
Liu, L., Liu, Y., Gao, F., et al. (2012). Embryonic development and gene expression of porcine SCNT embryos treated with sodium butyrate. J Exp Zool. Part B, Mol Dev Evol. 318, 224-234.

Maalouf, W.E., Alberio, R. and Campbell, K.H. (2008). Differential acetylation of histone H4 lysine during development of in vitro fertilized, cloned and parthenogenetically activated bovine embryos. Epigenetics. 3, 199-209.

Maalouf, W.E., Liu, Z., Brochard, V., et al. (2009). Trichostatin A treatment of cloned mouse embryos improves constitutive heterochromatin remodeling as well as developmental potential to term. BMC Dev Biol. 9, 11.

McGraw, S., Robert, C., Massicotte, L., et al. (2003). Quantification of histone acetyltransferase and histone deacetylase transcripts during early bovine embryo development. Biol Reprod. 68, 383-389.

Meirelles, F.V., Caetano, A.R., Watanabe, Y.F., et al. (2004). Genome activation and developmental block in bovine embryos. Anim Reprod Sci. 82-83, 13-20.

Mori, M., Otoi, T. and Suzuki, T. (2002). Correlation between the cell number and diameter in bovine embryos produced in vitro. Reprod Domest Anim. 37, 181-184.

Nakajima, H., Kim, Y.B., Terano, H., et al. (1998). FR901228, a potent antitumor antibiotic, is a novel histone deacetylase inhibitor. Exp Cell Res. 241, 126-133.

Pazin, M.J. and Kadonaga, J.T. (1997). What's up and down with histone deacetylation and transcription? Cell. 89, 325-328.

Pham, H., Ferrari, R., Cokus, S.J., et al. (2007). Modeling the regulatory network of histone acetylation in Saccharomyces cerevisiae. Mol Syst Biol. 3, 153.

Rice, J.C. and Allis, C.D. (2001). Histone methylation versus histone acetylation: new insights into epigenetic regulation. Cur Opin Cell Biol. 13, 263-273.

Robin, P., Fritsch, L., Philipot, O., et al. (2007). Post-translational modifications of histones H3 and H4 associated with the histone methyltransferases Suv39h1 and G9a. Genome Biol. 8, R270.

Rybouchkin, A., Kato, Y. and Tsunoda, Y. (2006). Role of histone acetylation in reprogramming of somatic nuclei following nuclear transfer. Biol Reprod. 74, 1083-1089.

Sawai, K., Fujii, T., Hirayama, H., et al. (2012). Epigenetic status and full-term development of bovine cloned embryos treated with trichostatin A. J Reprod Dev. 58, 302-309.

Schiltz, R.L., Mizzen, C.A., Vassilev, A., et al. (1999). Overlapping but distinct patterns of histone acetylation by the human coactivators p300 and PCAF within nucleosomal substrates. J Biol Chem. 274, 1189-1192.
Shi, L. and Wu, J. (2009). Epigenetic regulation in mammalian preimplantation embryo development. Reprod Biol Endocrinol : 7, 59.

Shi, L.H., Miao, Y.L., Ouyang, Y.C., et al. (2008). Trichostatin A (TSA) improves the development of rabbit-rabbit intraspecies cloned embryos, but not rabbit-human interspecies cloned embryos. Dev Dyn : 237, 640-648.

Suteevun, T., Parnpai, R., Smith, S.L., et al. (2006). Epigenetic characteristics of cloned and in vitro-fertilized swamp buffalo (Bubalus bubalis) embryos. J Anim Sci. 84, 2065-2071.

Taniguchi, M., Ikeda, A., Arikawa, E., et al. (2007). Effect of cryoprotectant composition on in vitro viability of in vitro fertilized and cloned bovine embryos following vitrification and in-straw dilution. J Reprod Dev. 53, 963-969.

Thongphakdee, A., Kobayashi, S., Imai, K., et al. (2008). Interspecies nuclear transfer embryos reconstructed from cat somatic cells and bovine ooplasm. J Reprod Dev. 54, 142-147.

Tribus, M., Galehr, J., Trojer, P., et al. (2005). HdaA, a major class 2 histone deacetylase of Aspergillus nidulans, affects growth under conditions of oxidative stress. Eukaryot Cell. 4, 1736-1745.

Wang, F., Kou, Z., Zhang, Y., et al. (2007). Dynamic reprogramming of histone acetylation and methylation in the first cell cycle of cloned mouse embryos. Biol Reprod. 77, 1007-1016.

Wittayarat, M., Sato, Y., Do, L.T., et al. (2013). Histone deacetylase inhibitor improves the development and acetylation levels of cat-cow interspecies cloned embryos. Cell Reprogr. 15, 301-308.

Wu, X., Li, Y., Xue, L., et al. (2011). Multiple histone site epigenetic modifications in nuclear transfer and in vitro fertilized bovine embryos. Zygote. 19, 31-45.

Xue, K., Song, J., Wei, H., et al. (2010). Synchronous behaviors of CBP and acetylations of lysine 18 and lysine 23 on histone H3 during porcine oocyte first meiotic division. Mol Reprod Dev. 77, 605-614.

Yamanaka, K., Sugimura, S., Wakai, T., et al. (2009). Acetylation level of histone H3 in early embryonic stages affects subsequent development of miniature pig somatic cell nuclear transfer embryos. J Reprod Dev. 55, 638-644.

Yamochi, T., Kida, Y., Oh, N., et al. (2012). Development of interspecies cloned embryos reconstructed with rabbit (Oryctolagus cuniculus) oocytes and cynomolgus monkey (Macaca fascicularis) fibroblast cell nuclei. Zygote. 1-9.

Zhang, Y., Li, J., Villemoes, K., et al. (2007). An epigenetic modifier results in improved in vitro blastocyst production after somatic cell nuclear transfer. Cloning Stem Cells. 9, 357-363.
Zhao, J., Ross, J.W., Hao, Y., et al. (2009). Significant improvement in cloning efficiency of an inbred miniature pig by histone deacetylase inhibitor treatment after somatic cell nuclear transfer. Biol Reprod. 81, 525-530.

Figure legends

Fig. 1. Immunolocalisation of acetylation on H3K9 (H3K9ac) (A), H3K18 (H3K18ac) (B), and H3K23 (H3K23ac) (C); dimethylation on H3K9 (H3K9me2) (D), and histone H3 (E) in the 2 h PF/PI, 6 h PF/PI, PN, 2-cell, 4-cell, and 8-cell stages of iSCNT cat embryos treated without (left, control) or with 50 nM TSA (middle) in comparison with *in vitro* fertilised bovine embryos (right). Each sample was counterstained with DAPI to visualise DNA. The pattern of H3K9/18/23ac and H3K9me2 were uniform between nuclei within the same embryo. Scale bar = 50 μm.

Fig. 2. Relative intensity levels of acetylation on H3K9 (H3K9ac) (A), H3K18 (H3K18ac) (B), H3K23 (H3K23ac) (C), di-methylation on H3K9 (H3K9me2) (D), and histone H3 (E) in the 2 h PF/PI, 6 h PF/PI, PN, 2-cell, 4-cell, and 8-cell stages of iSCNT cat embryos treated without or with 50 nM TSA in comparison to *in vitro* fertilised bovine embryos. Seven to ten iSCNT cat embryos with each staining were used to estimate the levels of H3K9/18/23ac, H3K9me2 and histone H3. Each bar represents the mean ± SEM. $^{a\text{-}c}$ represent significant differences ($p < 0.05$).

(B)

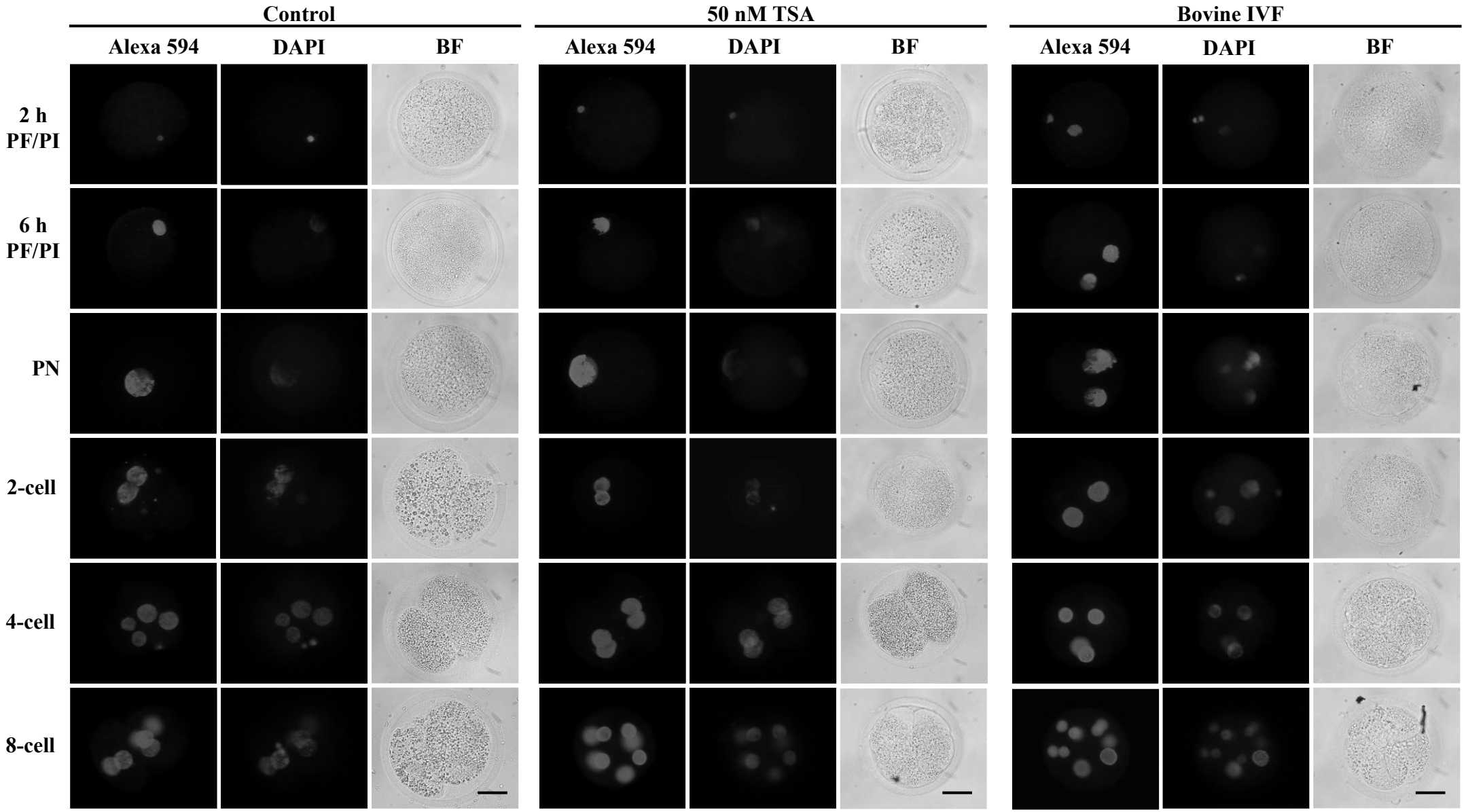
Control
50 nM TSA
Bovine IVF
Alexa 594
DAPI
BF
2 h PF/PI
6 h PF/PI
PN
2-cell
4-cell
8-cell